Supporting Information

Chemical Upcycling of Polybutadiene into Polyolefin-based dynamic Covalent Polymer Networks

Vincent Scholiers, Christophe Vos, Johan M. Winne, Dirk De Vos and Filip E. Du Prez

Table of contents

Materials and Instrumentation 2
Organocatalysis to obtain well-defined α,ω-dienes 6
Partial hydrogenation of high molar mass PBD-200k 6
Ethenolysis of hydrogenated PBD-200k 8
Monomer Synthesis and Characterisation 10
Concentrated solution of α,ω-dienes 10
Bisfunctional thiol (ODT): 1,8-Octanedithiol 11
Multifunctional thiol (X1): 2,2',2''-(cyclohexane-1,2,4-triyl)tris(ethane-1-thiol) 13
BrsO4 15
Material Synthesis and Characterisation 18
Synthesis protocol 18
FTIR 18
Swelling tests 19
DSC analysis 20
TGA analysis 21
Rheology 23
Tensile tests 25
Pictures 26
References 27

Materials and Instrumentation

Materials

Ammonium chloride (NH_4Cl, Carl Roth, ≥ 99%), sodium bicarbonate ($NaHCO_3$, Carl Roth, ≥ 99%), potassium carbonate (K_2CO_3, Carl Roth, ≥ 99%), sodium sulphate (Na_2SO_4, Carl Roth, ≥ 99%), hydrochloric acid (HCl, Chem-lab, 36%), chloroform-d (Eurisotop, 99.80%), dichloromethane (DCM, Fischer Chemicals, ≥ 99%), n-alkane standard mix C_7-C_{30} (Sigma Aldrich), 4-bromobenzenesulfonyl chloride (BrsOCl, Sigma Aldrich, 98%), 2,2-dimethoxy-2-phenlacetophenone (DMPA, Sigma Aldrich, 99%), ethyl vinyl ether (Sigma Aldrich, 99%), Grubbs Catalyst M202 (Sigma Aldrich), montmorillonite K 10 (Sigma Aldrich), polybutadiene (PBD, Sigma Aldrich, average M_w of 200-300 kDa; with 98% cis-1,4 addition), sodium hydroxide (NaOH, Sigma Aldrich, ≥ 97%), triethylamine (TEA, Sigma Aldrich, ≥ 99%), 1-butanol (TCI chemicals, 99%), 1,7-octadiene (TCI chemicals, 97%), $Ru(PPh_3)_3Cl_2$ (TCI chemicals, > 90%), thioacetic acid (TCI chemicals, > 95%), 1,2,4-trivinylcyclohexane (TVC, mixture of isomers, TCI Chemicals, >97%), diethyl ether (Et_2O, Thermo Scientific Chemicals), ethanol (EtOH, Thermo Scientific Chemicals, 96%), methanol (MeOH, Thermo Scientific Chemicals, 99.8%), cyclopentyl methyl ether (CPME, technical grade), ethyl acetate (EtOAc, technical grade), pentane (technical grade) were used as received. Azobisisobutyronitrile (AIBN, Janssen Chimica, ≥ 99%) was recrystallized two times before use.

Nuclear Magnetic Resonance (NMR) spectroscopy

High-field NMR spectra were recorded on a Bruker Avance III HD 400 or Bruker Ascend 400 spectrometer with a Bruker AscendTM 400 magnet system (^1H basic frequency of 400.17 MHz) and a 5 mm PABBO BB/19F-1H/D probe with z-gradients. All samples were dissolved in chloroform-d ($CDCl_3$). Data were recorded at room temperature using Bruker TopSpin 3.6.5 and processed and analyzed using Mestrenova 12.0.2. ^1H data were calibrated using tetramethylsilane (TMS) as an internal calibration reference. Chemical shifts (δ) are expressed in parts per million (ppm).

Gas Chromatography (GC)

GC analysis was performed on a Shimadzu GC-2010 Pro equipped with a CP Sil-5 CB column and an FID detector. An aliquot (200 µL) of the reaction mixture after ethenolysis or after purification was transferred to a vial for GC analysis. n-nonane (56 µmol, 10 µL), as the external standard, and ethyl vinyl ether (25 µL), to quench the catalyst, were added. 1µL of this sample was injected via an AOC-20i autosampler with a split ratio of 30. The N_2 carrier

gas had a total flow of 76.6 mL/min. The temperature vs time profile was as follows: 8 min. holding time at 35°C, ramp to 120°C with a rate of 7°C/min., a ramp to 280°C with a rate of 20°C/min. and lastly a holding time of 280°C for 10 min.

Gas Chromatography Mass Spectrometry (GC-MS)

The GC 6890N was equipped with a HP-1MS ultra inert column. 1 µL sample was injected with a split ratio of 30. The He carrier gas had a total flow of 1 mL/min. The temperature vs time profile was as follows: 4 min holding time at 40°C, ramp to 100°C with a rate of 5°C/min and a holding time of 2 min, a ramp to 280°C with a rate of 20°C/min and lastly a holding time of 5 min. The Agilent 5973N MSD was equipped with an electron impact ion source and a single quadrupole mass filter. A GC analysis was combined with a GC-MS analysis to identify the compounds. The retention times of the C_7-C_{30} n-alkanes in a standard mix were compared with the obtained retention times of the dienes to determine the chain lengths of products of C_{15} or higher.

Fourier-Transform Infrared spectroscopy (FTIR)

Measurements were recorded on a Perkin Elmer FTIR SPECTRUM 1000 spectrometer with Attenuated Total Reflection (ATR) with a PIKE Miracle ATR unit in a frequency range from 4000 to 600 cm^{-1}.

Thermogravimetric Analysis (TGA/DTGA)

Thermograms were recorded on a Mettler Toledo TGA/SDTA 851 under nitrogen atmosphere. Isothermal weight-loss measurements were conducted at a given temperature for 120 minutes whereas dynamic experiments used a heating rate of 10 K min^{-1} starting from 25 °C to 600 °C. The thermograms were analyzed using STARe software of Mettler-Toledo.

Differential Scanning Calorimetry (DSC)

DSC analyses were performed using a Mettler Toledo instrument 1/700 in nitrogen atmosphere with a heating and cooling rate of 10 K·min^{-1} starting from -100 °C to 100 °C. Glass transition temperatures (T_g) were determined from the second heating run on all samples to erase thermal history.

Swelling Degree and Soluble Fraction

Samples of ≈ 12 mg were brought into a vial and 3 mL of EtOAc was added and allowed to equilibrate for 48 h. Then, the solvent was removed, and the samples were dried *in vacuo* for 24 h at 60 °C. Each test was repeated fourfold to compensate for experimental errors. The gel

fraction was calculated using Equation S1 and the swelling degree was calculated using Equation S2, with m_i, m_s, and m_d representing the initial, swollen and dry mass, respectively.

$$Gel\ Fraction\ [\%] = 1 - \frac{m_i - m_d}{m_i} \quad \text{Equation S1}$$

$$Swelling\ Degree\ [\%] = \frac{m_s - m_i}{m_i} \quad \text{Equation S2}$$

Rheology

Rheological measurements were performed on an Anton Paar MCR 302 in a parallel plate geometry using 8 mm sample disks that were obtained with a hollow puncher of Boehm. ***Amplitude sweep*** measurements were performed at 90°C with a frequency of 1 rad/s, a constant normal force of 1 N and a shear strain which logarithmically increases from 0.01% to 10%. ***Stress relaxation*** experiments were performed between 140 and 100 °C with -10 °C intervals, applying a constant shear strain of 1% (within the LVE-region of the samples) and a constant normal force of 1 N. ***Frequency sweep*** experiments were also conducted with a constant normal force of 1 N, constant shear strain of 1% and the frequency was varied between 0.01 to 100 rad/s at different temperatures (140 to 100 °C, with -10 °C intervals).

The apparent flow activation energy ($E_{act,flow}$) from the stress relaxation experiments was determined by fitting the observed relaxation times (τ) to the Arrhenius equation Equation S3:

$$ln\tau = \frac{E_{act,flow}}{RT} + intercept \quad \text{Equation S3}$$

Where T is the temperature, and R is the gas constant.

Tensile Tests

Uniaxial tensile experiments were performed on a Tinius-Olsen H10KT tensile tester, equipped with a 100 N load cell and at a speed of 10 mm/min and a preload of 0.1 N. Flat dog-bone type specimens with an effective gauge length of 12 mm, a width of 2 mm, and a thickness of ± 0.8 mm were used for the tensile tests. Each tensile test was conducted at 40 °C. The samples were cut out by using a Ray-Ran dog-bone cutter. Additionally, an INSTRON alignment kit was used to align the grips. The tensile data were registered by using a National Instruments C-series data acquisition card. The signals from strain gauges as well as the load, displacement, and strain recorded by the FastTrack controller were measured on the same time basis. To obtain reproducible results, each experiment was repeated at least three times. The Young Modulus was calculated by linear regression from the stress–strain curve from 1% to 8% strain and the toughness from the area under the stress-strain curve.

(Re)processing

The materials were (re)processed by compression molding at 135 °C and 2 metric ton, for 30 minutes. The networks were cut into small pieces (± 2x2 mm) and put in a mold and compression molded. After this, the mold was taken out of the hot press and allowed to slowly cool to room temperature.

Organocatalysis to obtain well-defined α,ω-dienes

A procedure identical to literature was followed.[1]

Partial hydrogenation of high molar mass PBD-200k

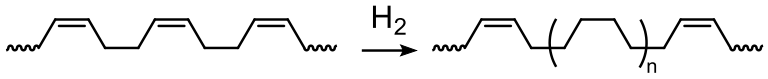

The hydrogenation of the high molar mass PBD was performed in a 600 mL Parr reactor. A stock solution of 1.2 M PBD-200k (based on a butadiene repeat unit of 54 g/mol) was prepared in a volumetric flask of 250 mL by dissolving PBD-200k (300 mmol, 16.2 g PBD) in CPME (232 mL) to a total volume of 250 mL at 50 °C. The mixture was brought in the glass liner of the Parr reactor together with 360 mg of $Ru(PPh_3)_3Cl_2$ (0.375 mmol, 0.125 mol% vs the butadiene unit). The reactor was closed, and the 350 mL headspace was flushed with N_2 and loaded with 14.5 bar H_2. The reactor was heated to 100 °C and stirred at 500 rpm for 5 h. The partially hydrogenated PBD-200k was precipitated in 500 mL of MeOH as anti-solvent, spread out on a crystallization dish and dried overnight in a vacuum oven at 80 °C. 15.17 g of a brown rubbery solid was obtained. The product was analyzed by liquid ^{1}H-NMR analysis ($CDCl_3$, 400 MHz) at room temperature. YIELD = 94%

In **Figure S1**, the ^{1}H NMR of the partially hydrogenated PBD-200k (hPBD-200k) is given and in **Table S1**, a summary of the data and calculation is given. To calculate the amount of C=C per 100C (%C=C), all the signals in the ^{1}H NMR spectrum of the hPBD-200k were divided by their number of H-atoms per C-atom (Signal NMR/#H). From these values and their sum, the relative amount of the different C-atoms was calculated (% Signal). The sum of %Signal H_a/2 and %Signal H_b represents the %C=C (S4). Here this is 22.68/2*100% = 11.3%

$$\%\mathrm{C}=\mathrm{C} = \%Signal\frac{H_a}{2} + \%SignalH_b \qquad \text{Equation S4}$$

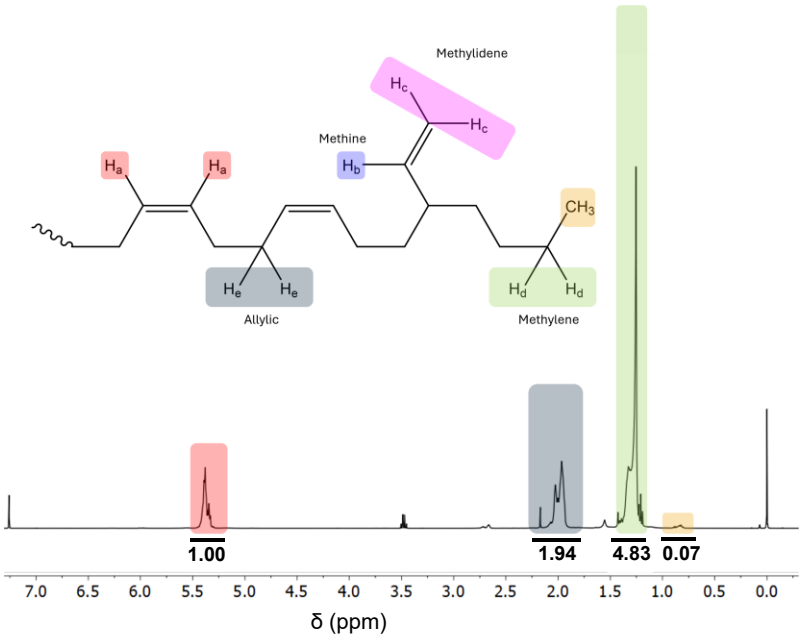

Figure S1. ^{1}H-NMR spectrum of hPBD-200k in $CDCl_3$.

Table S1. Summarized ^{1}H-NMR data of the hPBD-200k.

hPBD

Proton	Shift (ppm)	#H per C=C	Signal NMR	Signal NMR/#H	% Signal
H_b	5.5-5.8	1	**0.00**	0.00	**0.00**
H_a	5.25-5.5	1	**1.00**	1.00	**22.68**
H_c	4.8-5.25	2	**0.00**	0.00	0.00
H_e	1.8-2.4	2	1.94	0.97	22.00
H_d	1.2-1.55	2	4.83	2.42	54.78
CH_3	0.7-1	3	0.07	0.02	0.53
Total			7.84	4.41	100.0

Ethenolysis of hydrogenated PBD-200k

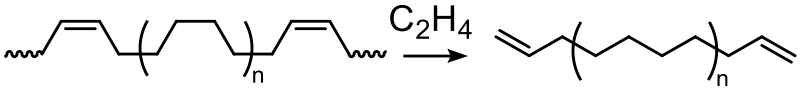

α,ω-dienes

Ethenolysis of hydrogenated PBD-200k (hPBD-200k) (1.5 g, 12 mmol double bonds, 1 eq.) was performed in $CDCl_3$ (30 mL) in a 60 mL Premex reactor. After stirring the PBD-$CDCl_3$ mixture overnight in a vial, undissolved particles were finely grounded using a mortar and pestle. The mixture was afterwards added to the reactor together with Grubbs Catalyst® M202 (0.0051 eq., 60 mg). After sealing the reactor, the headspace was purged with N_2 and loaded with 8 bar C_2H_4. The pressure was left to stabilize under magnetic stirring. The reactor was put in a preheated block of 80°C and magnetically stirred at 400 rpm for 2h. Another portion of Grubbs Catalyst® M202 (0.0034 eq., 40 mg) was added after cooling off the reactor in a water bath. The reaction was continued for another 2h under the same conditions. The grounding and extra addition steps were necessary to ensure high conversion during ethenolysis.

To purify the product mixture obtained after 4h, the contents of the reactor were transferred to a 50 mL falcon tube and 3g of montmorillonite K10 was added. The mixture was shaken vigorously and centrifuged at 5000 rpm for 1 minute. The liquid fraction was transferred to another falcon tube and 10 mL of $CDCl_3$ was added to the solid clay to extract leftover product. After shaking, the solid was centrifuged again and the two liquid fractions were added together. This process was repeated three times. After collecting all the liquid fractions, they were finally passed through an activated basic alox column for final purification.

To calculate the conversion of the internal C=C, the % signal of H_a was compared before and after ethenolysis. Conversion (X) was then calculated using Equation S5:

$$X = \frac{\%H_a\ before\ ethenolysis - \%H_a\ after\ ethenolysis}{\%H_a\ before\ ethenolysis} \times 100\% \qquad \text{Equation S5}$$

In this case: $X = \frac{22.68-2.68}{22.68} \times 100\% = 88\%$

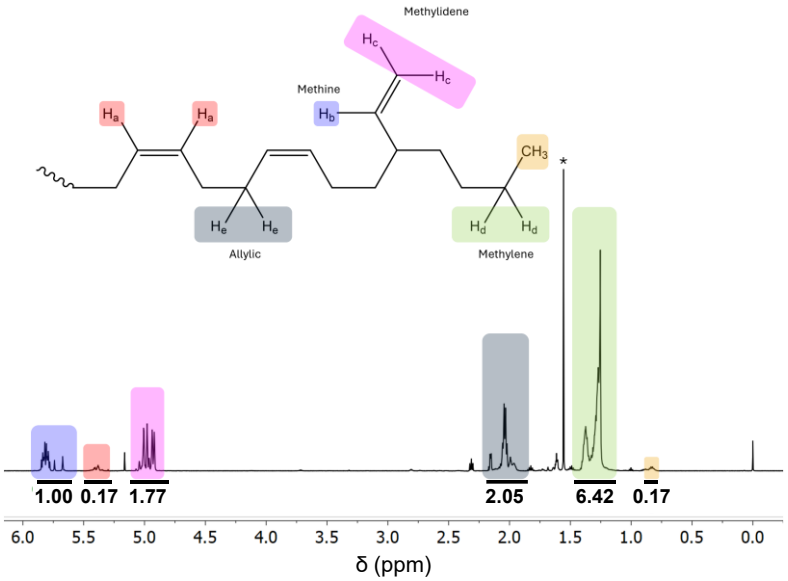

Figure S2. ^{1}H-NMR spectrum of hPBD-200k after ethenolysis in $CDCl_3$.

Table S2. Summarized ^{1}H-NMR data of the ethenolysis of the hPBD-200k.

Ethenolysis of hPBD

Proton	Shift (ppm)	#H per C=C	Signal NMR	Signal NMR/#H	% Signal
H_b	5.5-5.8	1	1.00	1.00	15.76
H_a	5.25-5.5	1	0.17	0.17	**2.68**
H_c	4.8-5.25	2	1.77	0.89	13.94
H_e	1.8-2.4	2	2.05	1.03	16.15
H_d	1.2-1.55	2	6.42	3.21	50.58
CH_3	0.7-1	3	0.17	0.06	0.89
Total			11.58	6.35	100.00

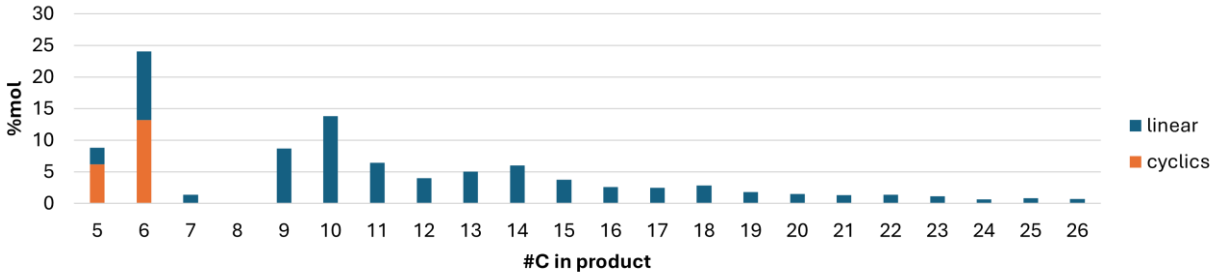

Figure S3. Product distribution after ethenolysis of partially hydrogenated PBD-200k with 11.4% C=C. Conditions: 1.5g partially hydrogenated PBD-200k in 30 mL $CDCl_3$, 100 mg Grubbs M202, 4h, 8 bar C_2H_4.

Monomer Synthesis and Characterisation

Concentrated solution of α,ω-dienes

The product from the ethenolysis of partially hydrogenated PB-200k was concentrated under reduced pressure (410 mbar at 40 °C) until around 40 wt%. of solvent remained. To determine the amount of double bonds in the solution, ^{1}H-NMR experiments were conducted using 1,3,5-trimethoxybenzene as an internal standard.

In a typical experiment:

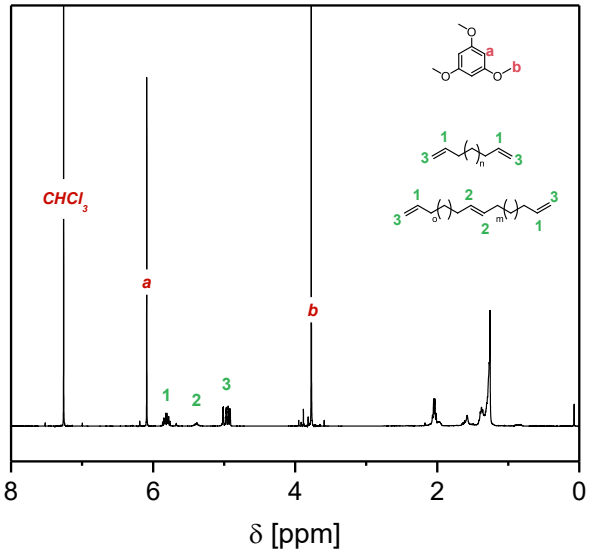

Determination double bonds/g

Shift (ppm)	#H	Signal NMR	#H
6.08 (a)	3	3	3
5.81 (1)	1	1.43	1
5.40 (2)	2	0.5	2
4.96 (3)	2	2.78	2

Total **#moles double bonds /g**	2.739 mmol/g
Percentage external double bonds	85 %

Figure S4. Determination of the total amount of double bonds/g in the concentrated solution of α,ω-dienes.

Experiments were conducted in fourfold to compensate for experimental errors. An average total of 2.73 ± 0.33 mmol/g double bonds was found of which 85 ± 0.5 % were external double bonds.

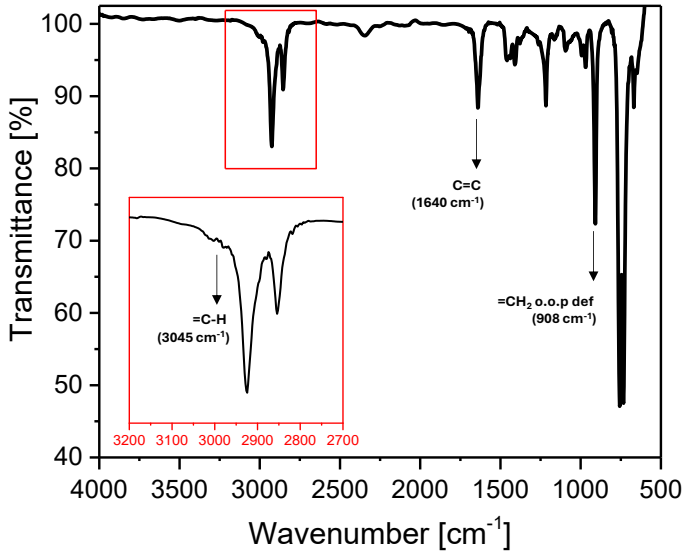

Figure S5. FTIR spectrum of the concentrated solution of α,ω-dienes with indicative vinyl stretching vibrations at 3045 cm^{-1}, 1640 cm^{-1} and 908 cm^{-1}.

Bisfunctional thiol (ODT): 1,8-Octanedithiol

A procedure identical to literature was followed.[2]

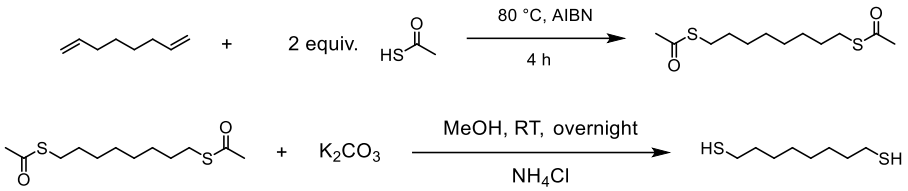

A 2-neck flask with a reflux cooler was filled with 1,7-octadiene (40 g, 0.36 mol), thioacetic acid (55.25 g, 0.73 mol) and AIBN (3.6 mmol), and was heated to 80 °C for 4h under inert atmosphere. Next, the mixture was diluted with Et_2O (350 mL) and washed with subsequently water (5 x 250 mL) and brine (250 mL). Finally, the organic phase was dried with Na_2SO_4 and evaporated in vacuo to yield octane-1,8-dithioacetate as a white/yellowish solid. This product was used in the next step without purification.

To a cooled solution of octane-1,8-dithioacetate in MeOH (15 g in 150 mL), K_2CO_3 (71.1 g, 9 equiv., 0.51 mol) was added. The resulting mixture was stirred at room temperature for 4 hours. Next, the solvent was partially evaporated after which $K_2CO_3$was quenched with a saturated NH_4Cl solution, and the desired product was extracted with Et_2O (3 x 100 mL). The combined organic layers were washed with water (150 mL), dried with Na_2SO_4 and evaporated in vacuo. The obtained product was purified by Kughelrohr distillation (220 °C). YIELD = 78 %.

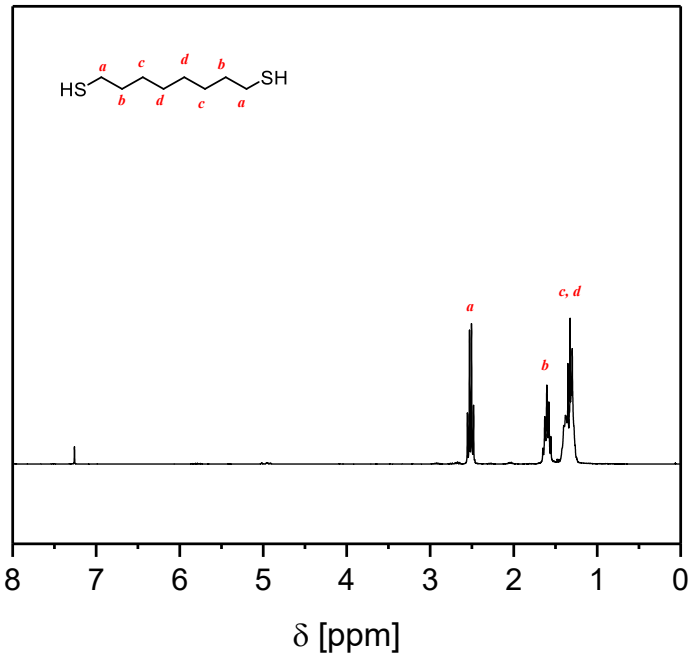

Figure S6. ^{1}H-NMR spectrum of ODT.

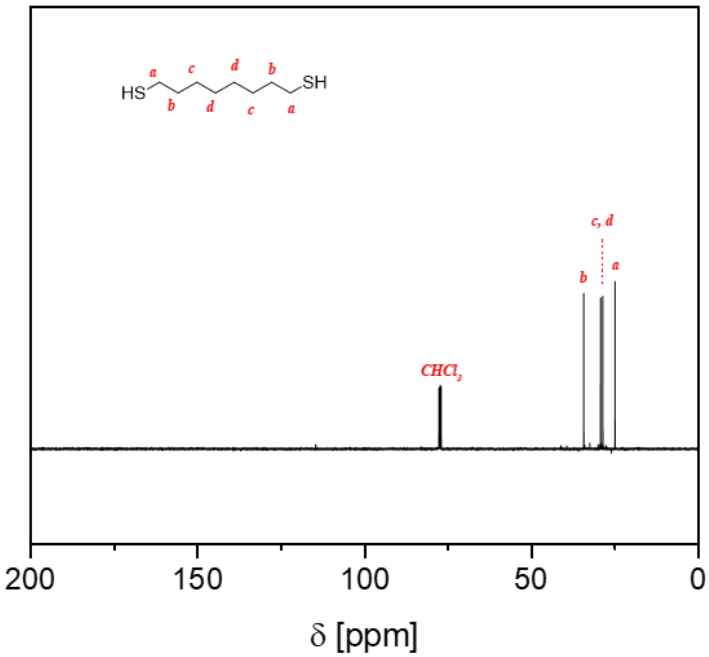

Figure S7. ^{13}C-NMR spectrum of ODT.

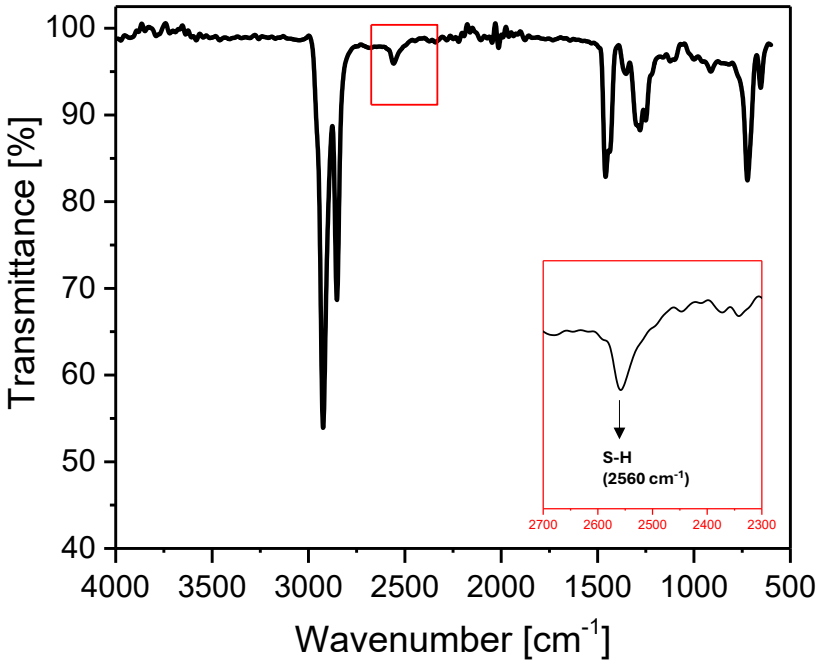

Figure S8. FTIR spectrum of ODT with indicative S-H stretching vibration (2560 cm^{-1}).

Multifunctional thiol (X1): 2,2',2''-(cyclohexane-1,2,4-triyl)tris(ethane-1-thiol)

A procedure identical to literature was followed.[3]

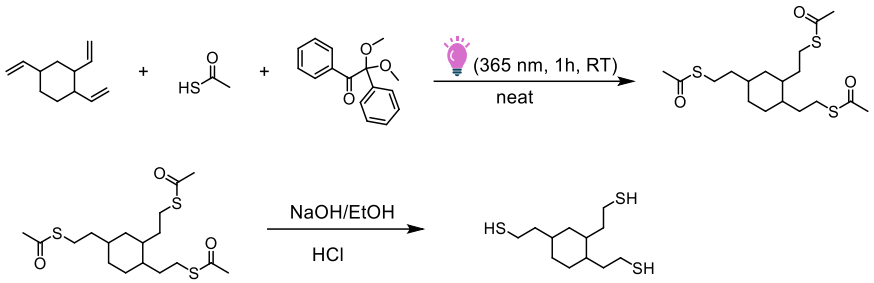

1,2,4-Trivinylcyclohexane (TVC, mixture of isomers, 50 mL, 0.26 mol) was cooled to -10 ◦C in an ice-salt bath in a 500 mL erlenmeyer flask. Under vigorous stirring and continued cooling in the ice-salt bath, thioacetic acid (60.75 mL, 0.775 mol) was slowly added, followed by 2,2-dimethoxy-2-phenylacetophenone (DMPA, 0.75 g, 1.95 mmol). An efficient reflux cooler was then fitted, followed by the removal of the ice-salt cooling bath. After the initial exotherm had subsided, the reaction mixture was brought under argon and was irradiated for 1 hour, using a custom-built photoreactor, fitted with 4 x 36 W UV lamps (Philips CLEO Compact PL-L (2G11), λ_{max} = 350 nm, λ-range: 310-400 nm).

Subsequently, the trithioacetate (5.0 g, 12.80 mmol) was dissolved in 15 mL EtOH and an NaOH solution was added in a drop-wise fashion (2.2 g, 55mmol in 6 mL of water) (solution turned dark red) and refluxed for 2 hours before cooling down to room temperature. The mixture was neutralized with HCl (1M, solution turned back to yellow) and extracted with Et_2O (2x30 mL). The organic phases were washed with water (2x15 mL), $NaHCO_3$ (2x15 mL) and brine (2x15 mL). The product was dried over Na_2SO_4, and concentrated under reduced pressure, yielding an orange/yellow oil that was further purified under high vacuum by Kugelrohr (250°C) to obtain a transparent oil with unpleasant smell. YIELD = 82%.

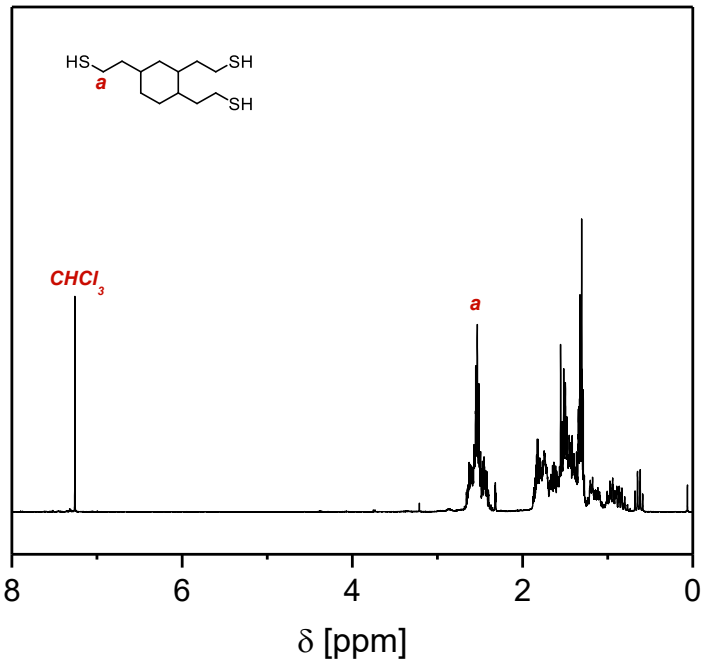

Figure S9. ^{1}H-NMR spectrum of ODT.

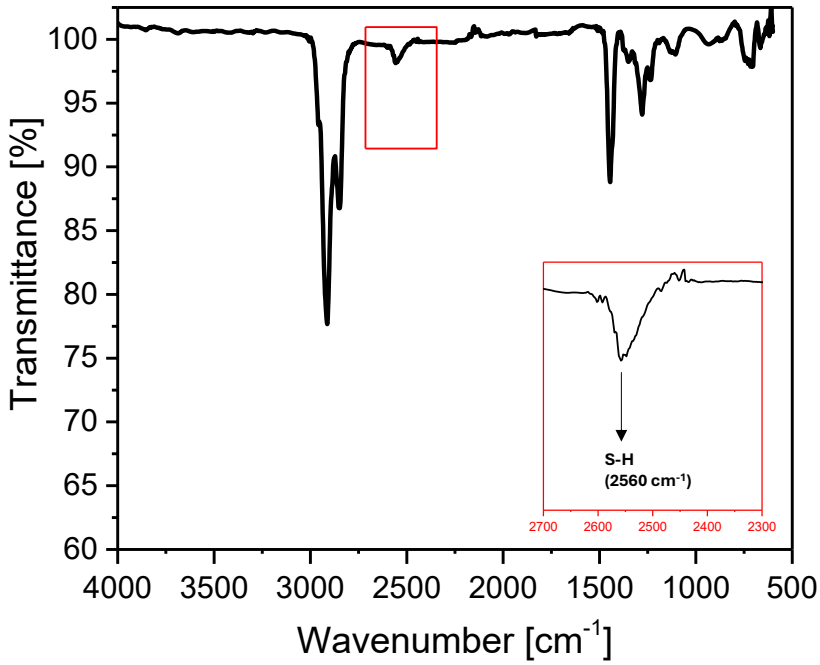

Figure S10. FTIR spectrum of X1 with indicative S-H stretching vibration (2560 cm^{-1}).

BrsO4

A procedure identical to literature was applied.[2]

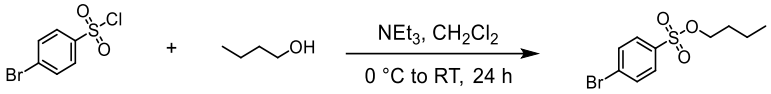

A 2-neck 500 mL round bottomed flask was loaded with a solution of 4-bromobenzenesulfonyl chloride (25.00 g, 97.84 mmol, 1.20 equiv.) in DCM (150 mL) and cooled to 0 °C in an ice-bath under argon atmosphere. Subsequently, 1-butanol (7.46 mL, 81.54 mmol, 1 equiv.) and triethylamine (22.73 mL, 163.07 mmol, 2 equiv.) dissolved in 100 mL DCM were added dropwise. The resulting mixture was then stirred at room temperature, and the reaction progress was monitored using thin-layer chromatography (TLC). Once the reaction was complete, the mixture was washed with water (2 x 250 mL), 1 M HCl (2 x 250 mL), saturated $NaHCO_3$ (2 x 250 mL) and brine (2 x 250 mL). The obtained organic phase was then dried with Na_2SO_4, and the solvent evaporated under reduced pressure. The product was purified by column chromatography using EtOAc/n-pentane (5/95) as eluent. YIELD = 92%.

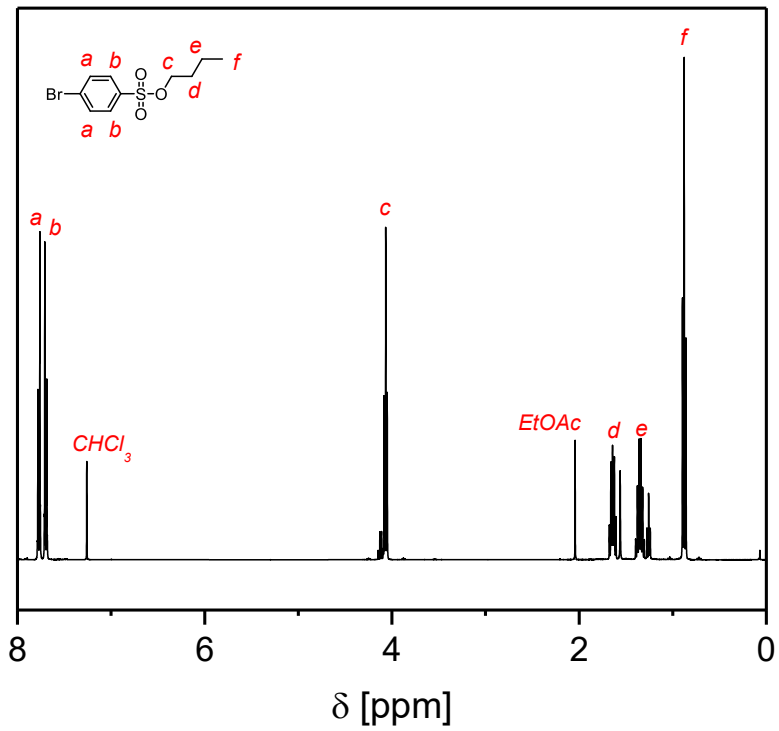

Figure S11. ^{1}H-NMR spectrum of BrsO4

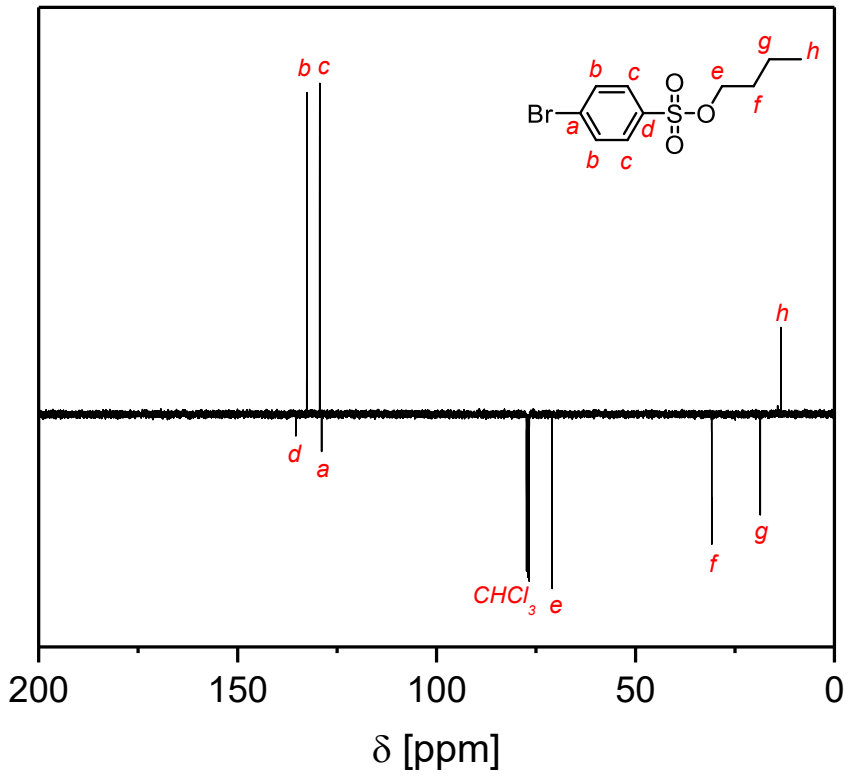

Figure S12. ^{13}C-NMR spectrum of BrsO4.

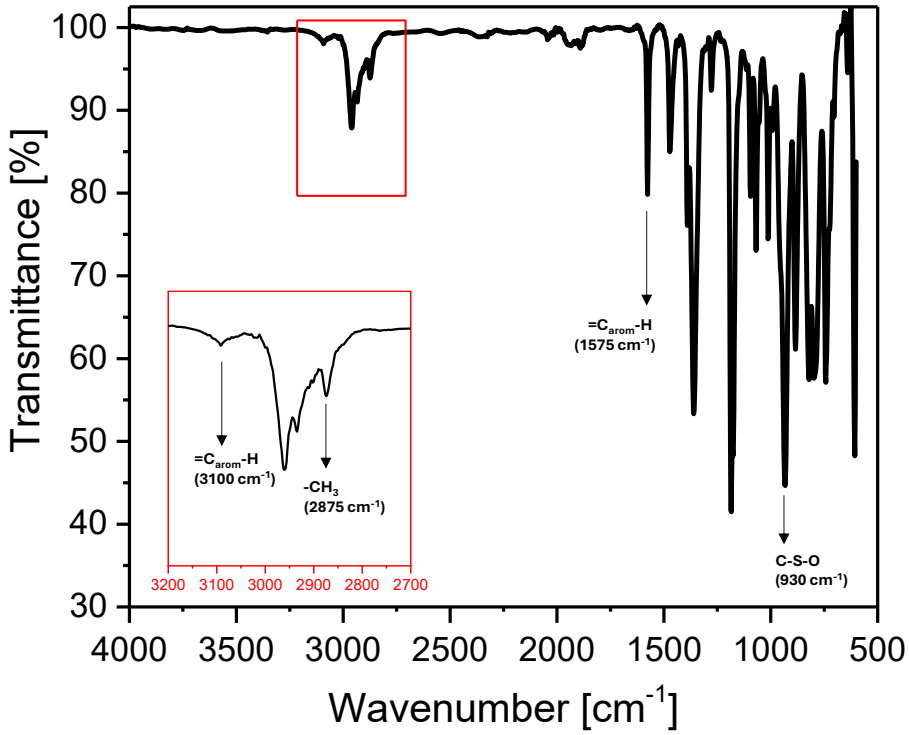

Figure S13. FTIR spectrum of BrsO4 with aromatic C-H stretch at 3100 cm^{-1} and aromatic ring stretch at 1575 cm^{-1}. Also visible is the -CH_3 stretch at 2875 cm^{-1} stemming from the butyl group and C-S-O stretch, indicating the presence of an intact sulfonate group.

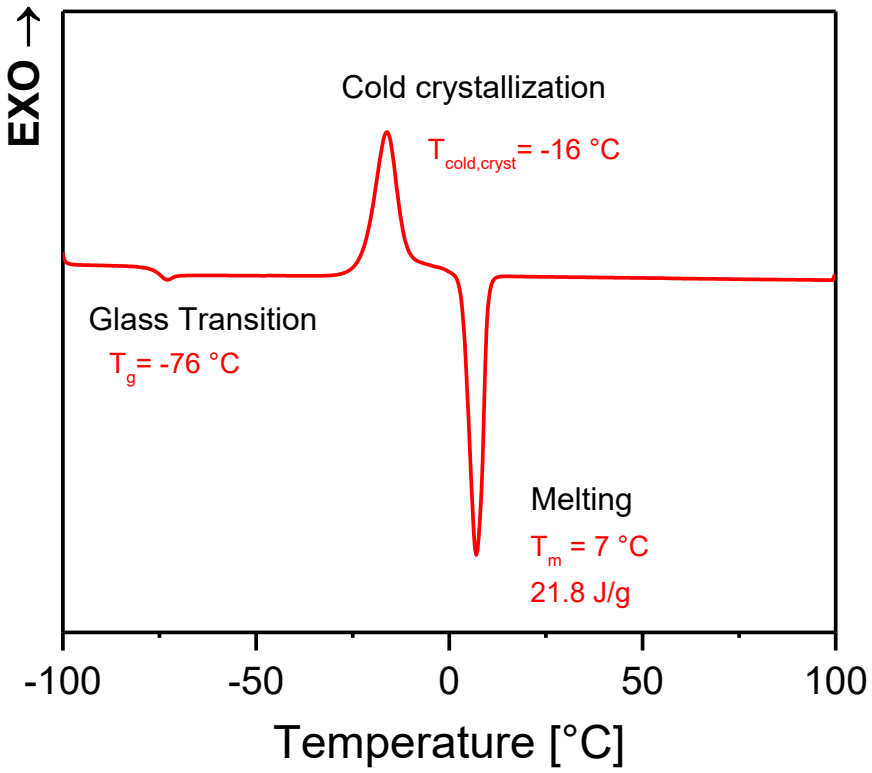

Figure S14. DSC thermogram of BrsO4, revealing a T_m at 7 °C.

Material Synthesis and Characterisation

Synthesis protocol

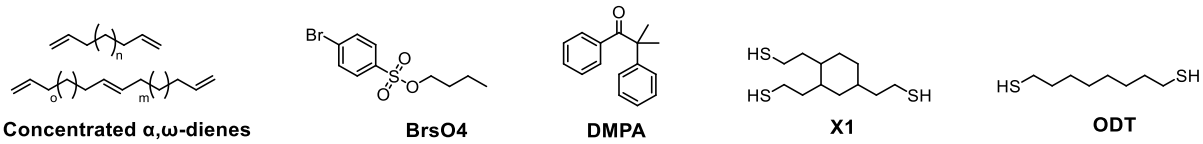

All upcycled PBD dynamic networks were prepared in a stoichiometric ratio between reactive SH functionalities and total amount of double bonds of the concentrated α,ω-dienes (index 100). In a typical experiment, the concentrated α,ω-dienes were mixed with X1, ODT, BrsO4 (10 mol% relative to formed thioether bonds, except for the reference sample) and 2,2-dimethoxy-2-phenylacetophenone (DMPA) (1mol%) in a pressure vial. The homogenous mixture is then cast into a mold consisting of two glass plates separated by a 1 mm thick silicone spacer and exposed to UV irradiation in a custom-made UV chamber (λ = 365 nm, 30 min). To ensure the covalent integration of the alkylating additive, the samples were placed in the vacuum oven at 40 °C after which the temperature was systematically increased up to 100 °C and kept at this temperature for 100 minutes. The resulting dried networks were then transferred to a mold and reshaped in a heating press (135 °C, 30 min, 2 tons/m^2) to create reproducible samples for characterization.

FTIR

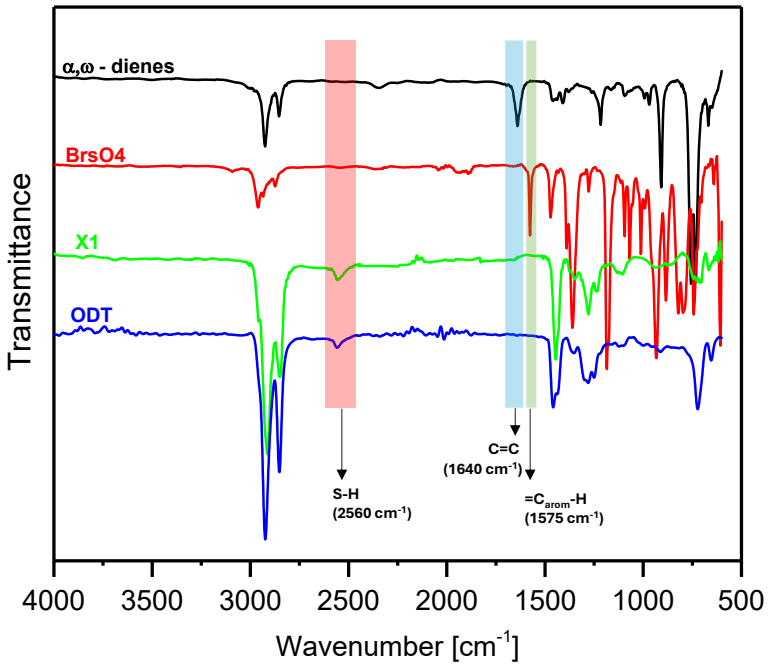

Figure S15. Stacked FTIR spectra of the monomers used in the resin formulation.

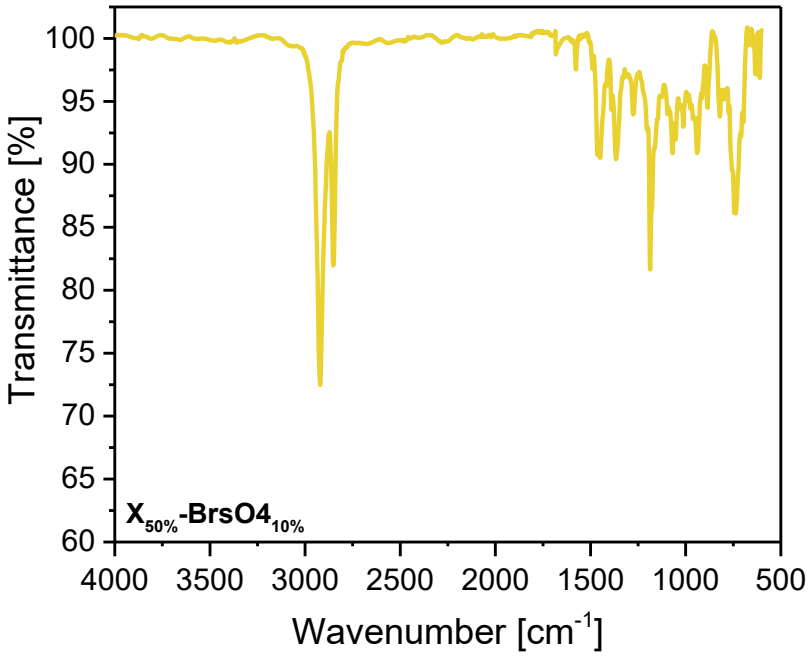

Figure S16. FTIR spectrum of $X_{50\%}$-$BrsO4_{10\%}$ acquired after the photochemical thiol-ene cure.

Swelling tests

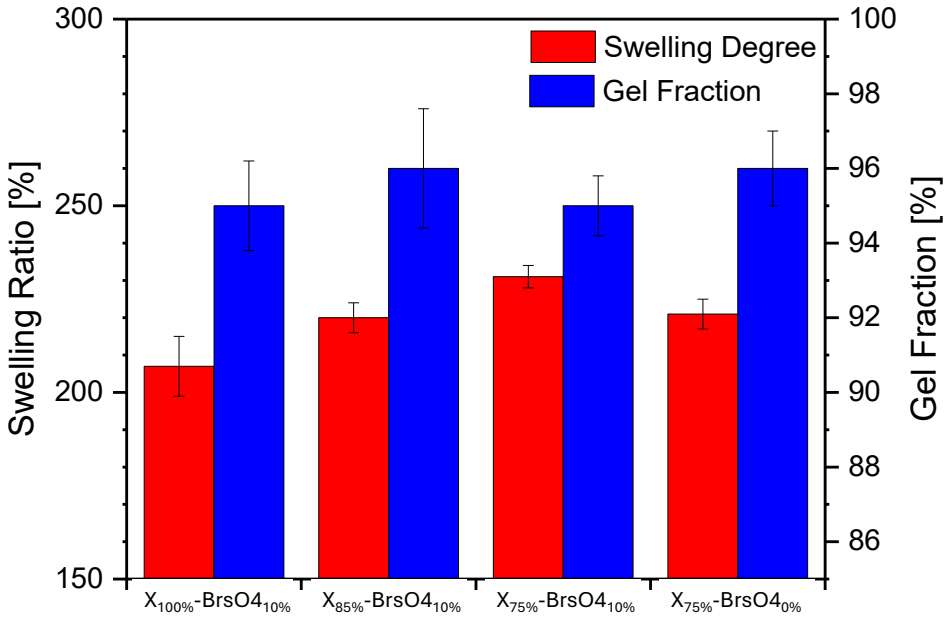

Figure S17. Swelling ratios and gel fractions of the prepared materials.

DSC analysis

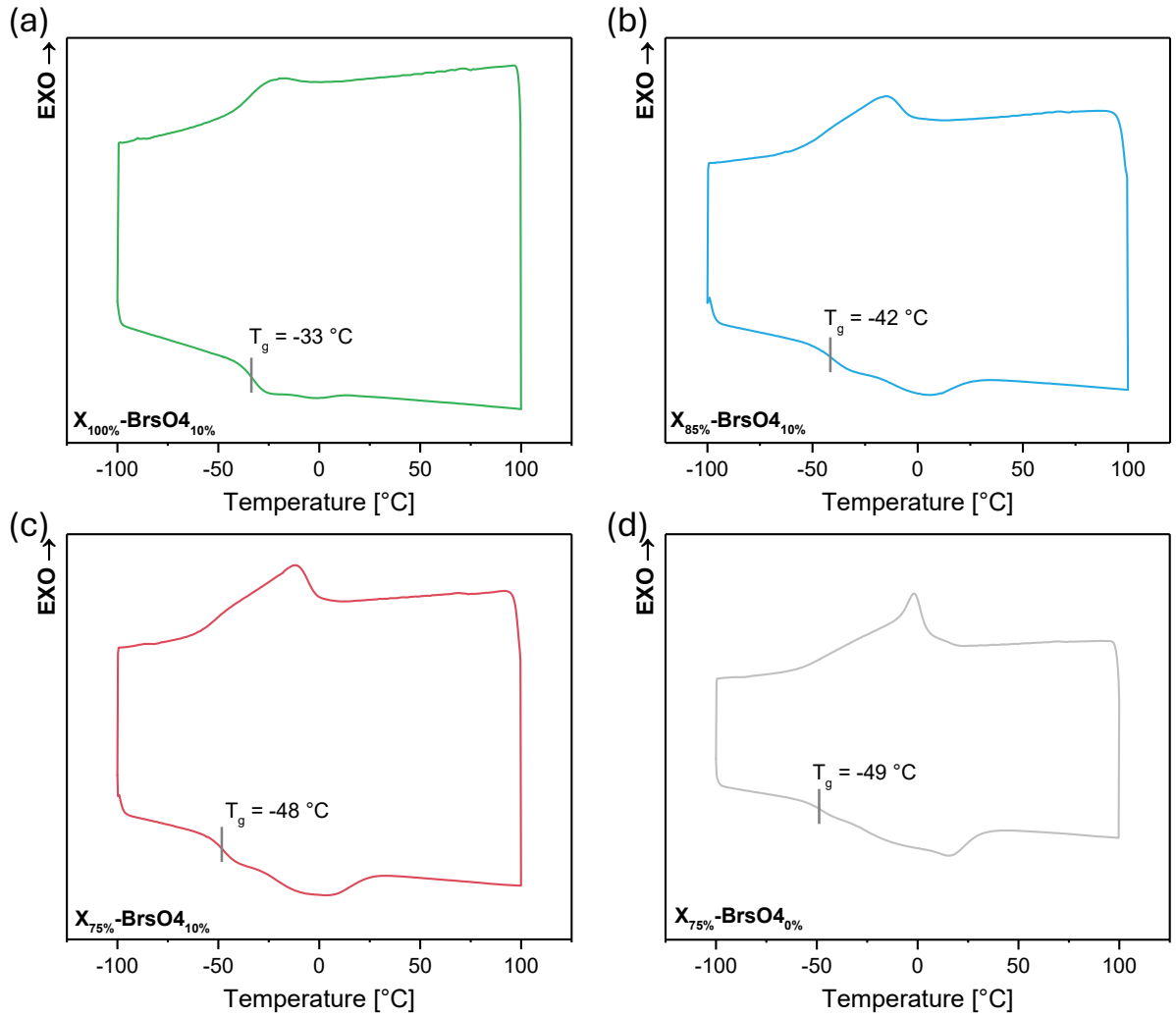

Figure S18. DSC thermograms of $X_{100\%}$-$BrsO4_{10\%}$ (a), $X_{85\%}$-$BrsO4_{10\%}$ (b), $X_{75\%}$-$BrsO4_{10\%}$ (c) and $X_{75\%}$-$BrsO4_{0\%}$ (d) containing the cooling and second heating runs. As the ODT content increases, corresponding to a decrease in cross-link density, the area under the exothermic peak during the cooling run becomes larger, indicating a higher fraction of crystalline domains formed within the material.

TGA analysis

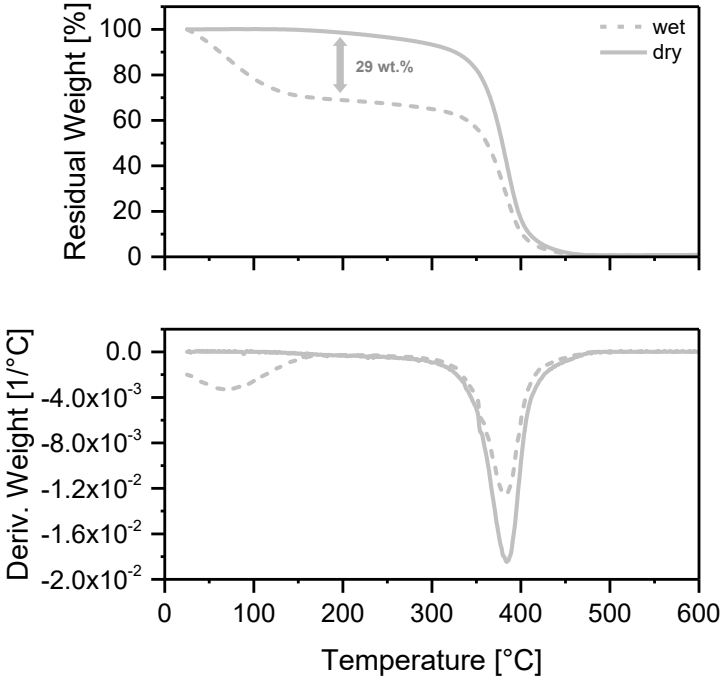

Figure S19: Dynamic TGA analysis of $X_{75\%}$-$BrsO4_{0\%}$ acquired before and after the post thermal cure, revealing a residual solvent content of 29 wt.% after the photochemical thiol-ene cure that is removed after the drying step (N_2 atmosphere and +10 °C/min heating rate).

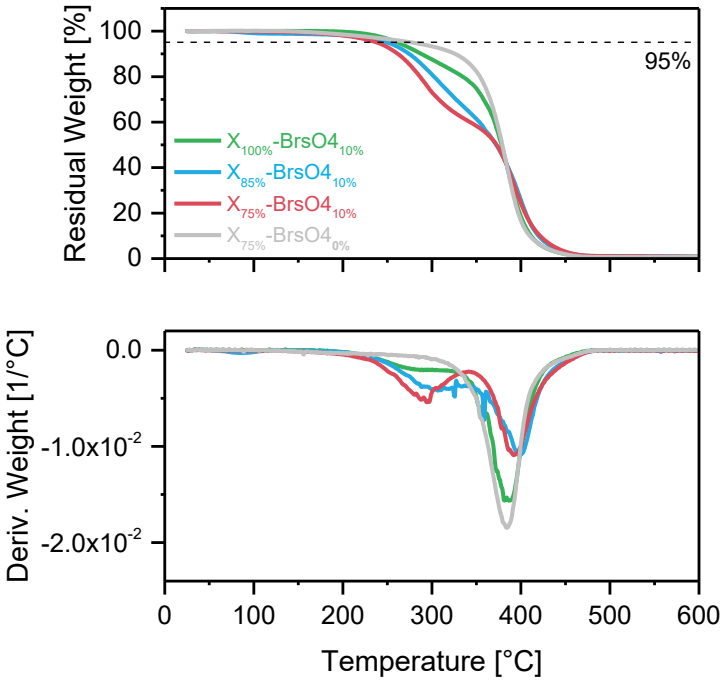

Figure S20. Dynamic TGA analysis of the upcycled PBD dynamic networks. All materials except for the reference material ($X_{75\%}$-$BrsO4_{0\%}$) exhibit a two-step degradation pattern. This is in line with other thermal analysis results of dynamic materials containing trialkylsulfonium salts.[2,4]

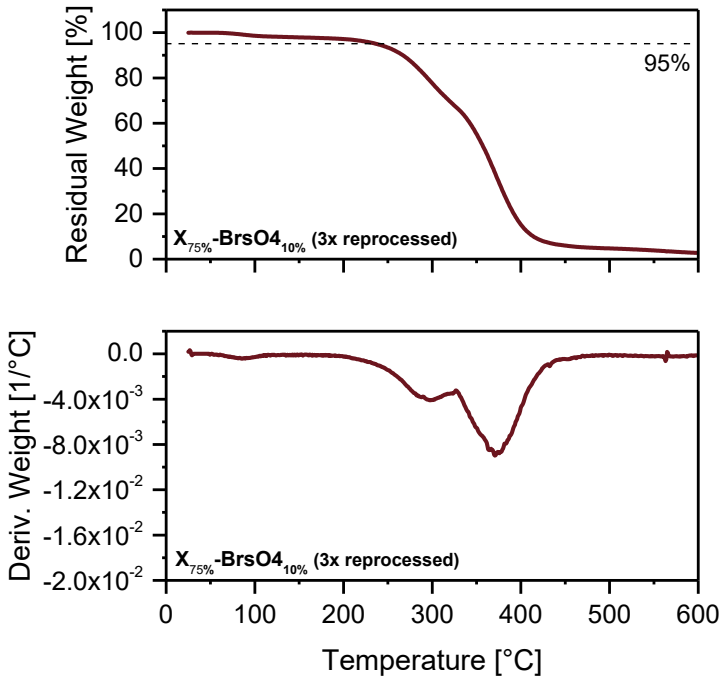

Figure S21. Dynamic TGA analysis of $X_{75\%}$-$BrsO4_{10\%}$ after being subjected to three iterative reprocessing cycles.

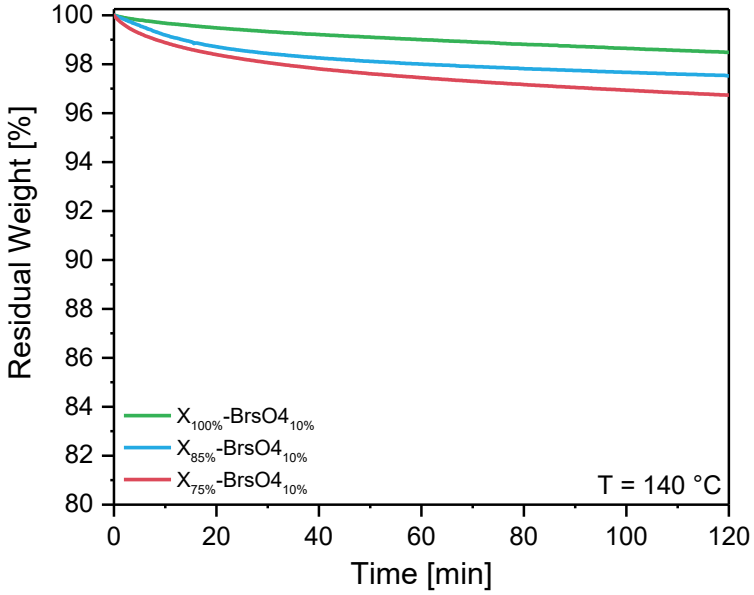

Figure S22. Isothermal TGA analysis measured at 140 °C of the upcycled PBD dynamic networks under N_2 atmosphere.

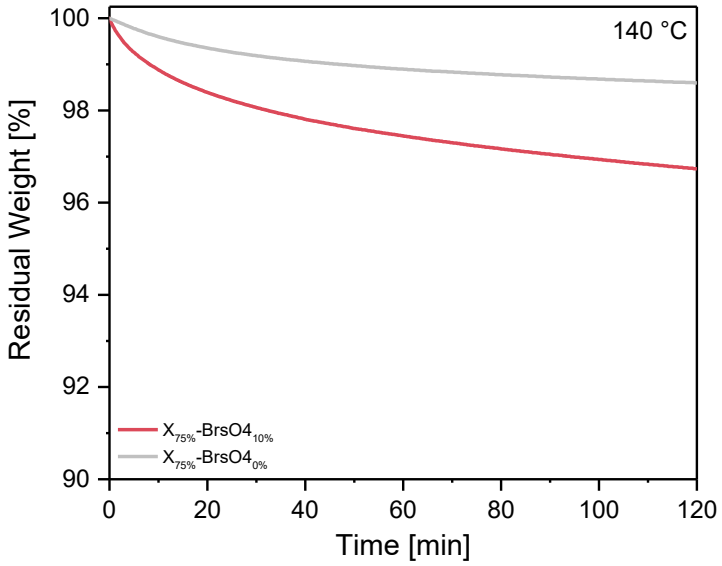

Figure S23. Isothermal TGA analysis measured at 140 °C under N_2 atmosphere of $X_{75\%}$-$BrsO4_{10\%}$ and $X_{75\%}$-$BrsO4_{0\%}$.

Rheology

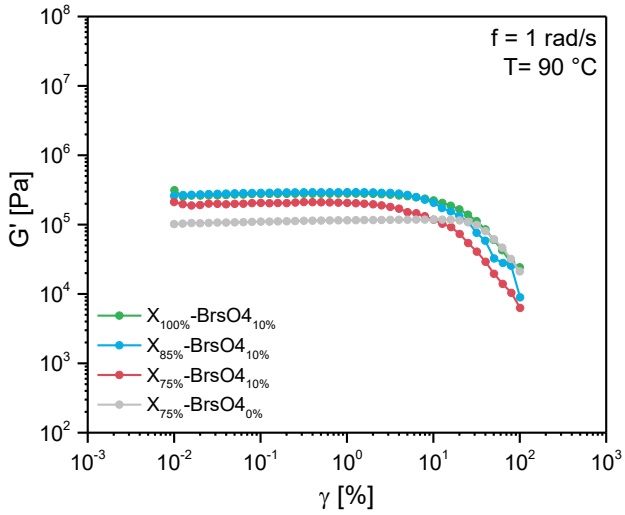

Figure S24. Amplitude sweeps measured at 90 °C with a fixed frequency of 1 rad/s and a constant normal force of 1N.

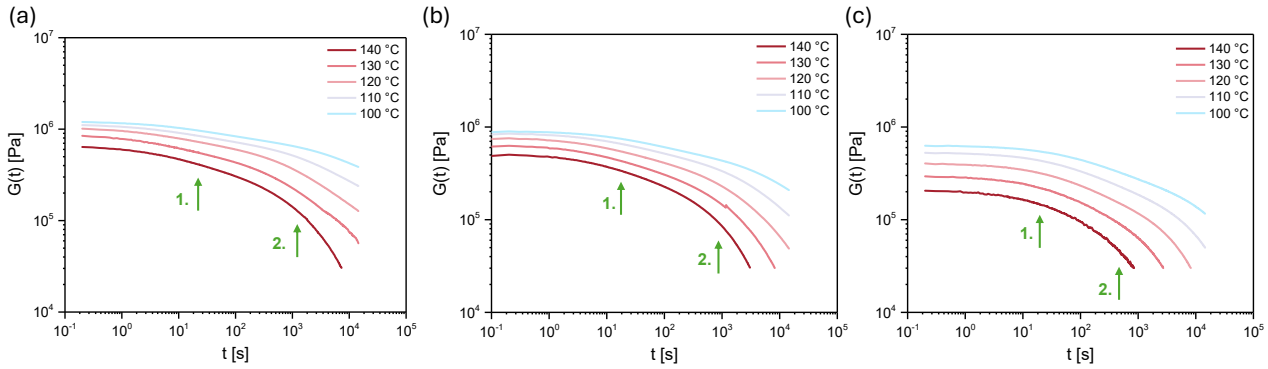

Figure S25. Non-normalised stress relaxation experiments recorded between 140 °C and 100 °C of $X_{100\%}$-$BrsO4_{10\%}$ (a), $X_{85\%}$-$BrsO4_{10\%}$ (b) and $X_{75\%}$-$BrsO4_{10\%}$ (c). Upon closer inspection, a double relaxation decay can be differentiated. At short time intervals (1.), stress relaxation is primarily governed by chain segments, entanglements, and loops. At longer timescales (2.), the relaxation behaviour is dominated by the dynamic exchange of thioether linkages.

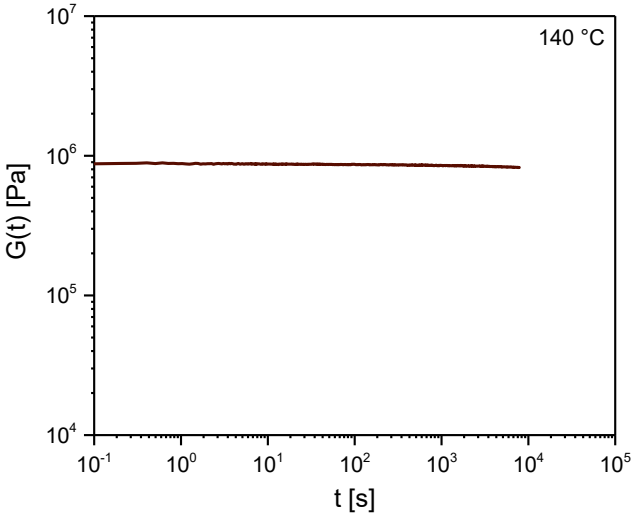

Figure S26. Stress relaxation curve at 140 °C of the reference material that contains no dynamic trialkylsulfonium groups ($X_{75\%}$-$BrsO4_{0\%}$), demonstrating the inability of the material to dissipate stress.

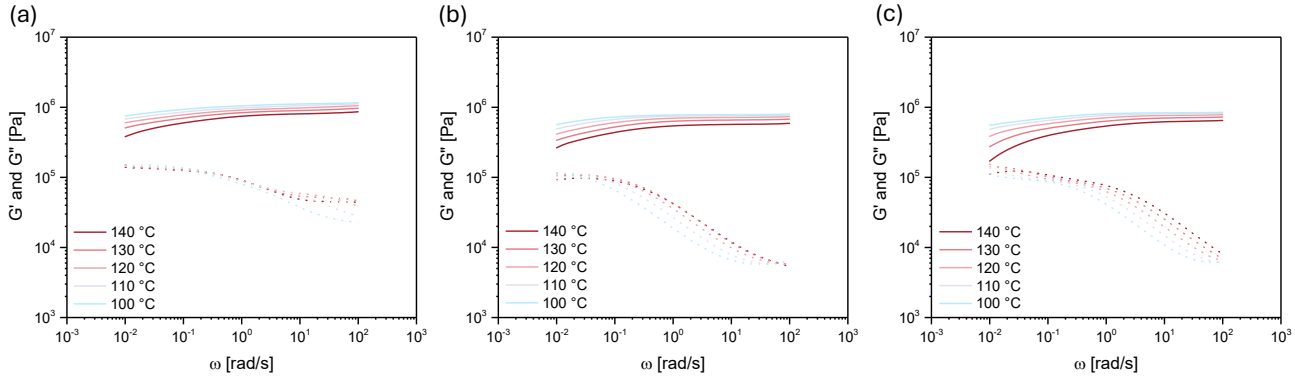

Figure S27. Frequency sweep spectra of $X_{100\%}$-$BrsO4_{10\%}$ (a), $X_{85\%}$-$BrsO4_{10\%}$ (b) and $X_{75\%}$-$BrsO4_{10\%}$ (c) measured between 140 °C and 100 °C.

Tensile tests

(a)

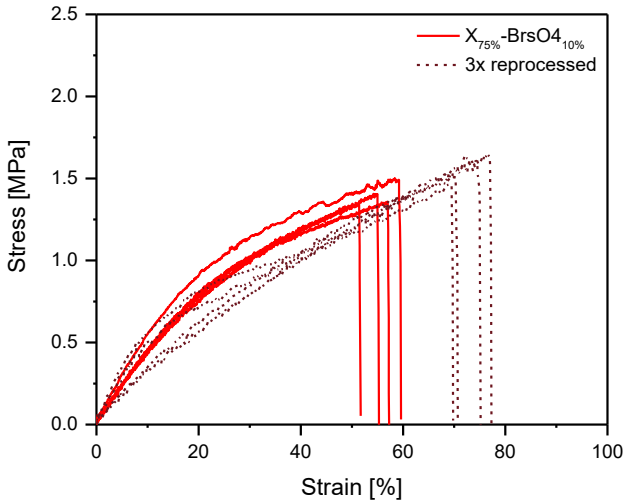

(b)

	Young Modulus [MPa]				Ultimate Tensile Strength (UTS) [MPa]			Strain At Break [%]			Toughness [MPa]		
	value	*error*	*average*	*error*	*value*	*average*	*error*	*value*	*average*	*error*	*value*	*average*	*error*
R0_I	4.49	0.02	4.56	0.43	1.36	1.40	0.06	56.90	55.63	2.86	0.51	0.51	0.06
R0_II	5.27	0.02			1.50			59.20			0.60		
R0_III	4.36	0.02			1.35			51.40			0.43		
R0_IV	4.12	0.02			1.41			55.00			0.48		
R3_I	3.26	0.02	4.25	1.05	1.64	1.57	0.08	74.40	72.63	3.15	0.71	0.69	0.03
R3_II	5.19	0.09			1.47			69.50			0.63		
R3_III	3.15	0.04			1.65			76.90			0.72		
R3_IV	5.41	0.08			1.51			69.70			0.68		

Figure S28. Tensile test conducted on $X_{75\%}$-$BrsO4_{10\%}$ before and after being subjected to 3 iterative reprocessing cycles. (a) Stress-strain curves. (b) Summary of the mechanical properties abstracted from the tensile tests.

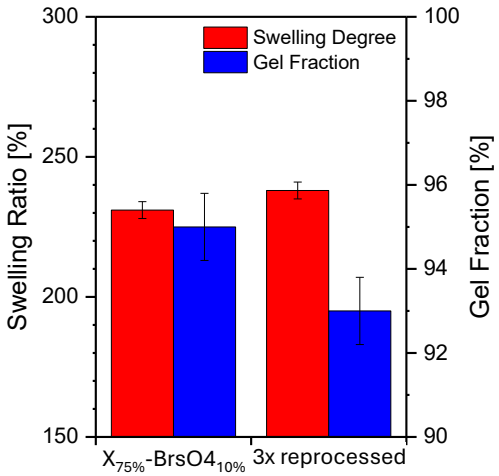

Figure S29. Swelling ratios and gel fractions of $X_{75\%}$-$BrsO4_{10\%}$ before and after being subjected to 3 iterative reprocessing cycles.

Pictures

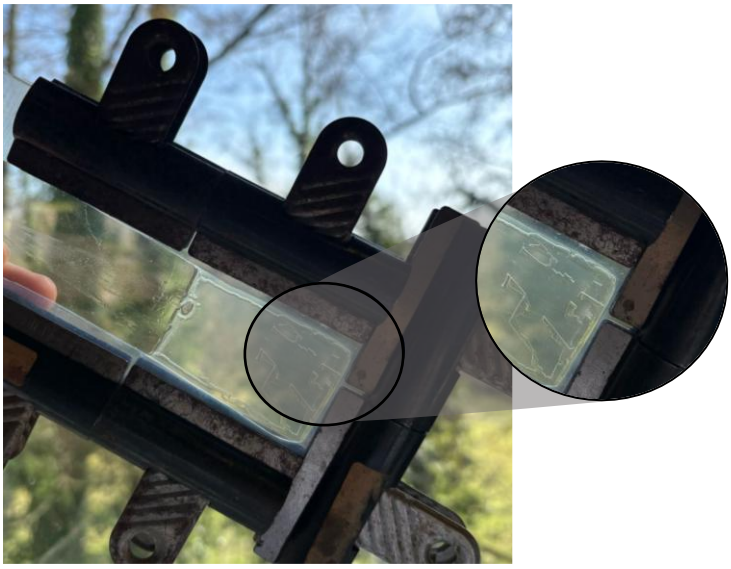

Figure S30. Picture of the reference material $X_{75\%}$-Brs$O4_{0\%}$ taken directly after being exposed to 30 minutes of UV irradiation (λ= 365 nm). Visible traces of residual solvent - stemming from the ethenolysis step - are released during photocuring due to the exothermic nature of the radical mediated thiol-ene reaction.



Figure S31. Picture of $X_{75\%}$-Brs$O4_{0\%}$ taken directly after the post-thermal cure in the vacuum oven (T= 100°C, Δt = 100 min).

References

[1] C. Vos, I. Beckers, G. O'Rourke, and D. De Vos, "Chemical Upcycling of Polybutadiene into Size Controlled α,ω-dienes and Diesters via Sequential Hydrogenation and Cross-metathesis," *Chemical Science* 16 (2025): 3544–3551, https://doi.org/10.1039/D4SC06826B.

[2] B. Hendriks, J. Waelkens, J. M. Winne, and F. E. Du Prez, "Poly(thioether) Vitrimers via Transalkylation of Trialkylsulfonium Salts," *ACS Macro Letters* 6 (2017): 930–934, https://doi.org/10.1021/acsmacrolett.7b00494.

[3] J. Van Damme, O. Van Den Berg, J. Brancart, et al., "Anthracene-Based Thiol–Ene Networks with Thermo-Degradable and Photo-Reversible Properties," *Macromolecules* 50 (2017): 1930–1938, https://doi.org/10.1021/acs.macromol.6b02400.

[4] V. Scholiers, S. M. Fischer, B. Daelman, et al., "Tailoring the Reprocessability of Thiol-Ene Networks through Ring Size Effects," *Angewandte Chemie International Edition* 64 (2025), https://doi.org/10.1002/anie.202420657.